Acta Materialia Transylvanica 1/2. (2018) 81–84.
https://doi.org/10.2478/amt-2018-0028
Hungarian: https://doi.org/10.2478/amt-2018-0027
https://eda.eme.ro/handle/10598/30463

Corrosion Testing of Additively Manufactured Metals and Biomedical Devices

Dávid Miklós KEMÉNY[1], Dóra KÁROLY[2]

Budapest University of Technology and Economics, Faculty of Mechanical Engineering, Department of Materials Science and Technology, Budapest, Hungary

[1] *kemenydavid@edu.bme.hu*

[2] *kdora@eik.bme.hu*

Abstract

Additive manufacturing (AM) is becoming increasingly important, making it possible to produce a product in a short time, to specific individual requirements, and even in the presence of the customer. This research is related to direct metal laser sintering of additive manufacturing. This new technology is increasingly being used in more sectors, for example in biomedical industry, where a damaged product can potentially endanger human life. Corrosion tests were carried out during our research. Cyclic voltammetry curves and corrosion rates were determined with a potentiostat. Two typical biocompatible implant materials were compared, a cobalt chromium alloy (powder metallurgy) and a titanium alloy (3D printed). The results will help in specifying the corrosion properties of additively manufactured materials.

Keywords: *additive manufacturing, direct metal laser sintering, corrosion, cyclic voltammetry*

1. Introduction

Nowadays, the use of additive manufacturing technologies is becoming more widespread. For this reason, complicated products can now be made precisely and quickly, even in the presence of the customer. With this technology, three-dimensional bodies can be created which are not possible or are too difficult to produce with conventional technology. This process was initially used with polymers, but today it can be applied to almost all raw materials: metals, plastics, ceramics, papers or a combination of these (composites) **[1, 2]**.

Before additive manufacturing, a 3D model is required, which is produced using CAD (Computer Aided Design) software and can, therefore, be changed at any time. Subsequently, the model is saved in the STL (Standard Tessellation Language) file format, thus linking the 3D software and the AM device. Using the STL file format, the surface of the body is approximated by triangles: the smaller the size the better the original geometry of the body. During the AM process, the desired product is built up layer-by-layer, based on the 3D CAD model **[1,2]**. The process of forming by the product is shown in **Figure 1.**

During this process, the powder diffuser disperses a layer of dust on the powder coating which is melted by a high-performance laser according to the desired geometry. As soon as a layer is completed, the pattern is lowered, the powder diffuser creates a new layer that the laser scans again, and this process repeats until the product is ready.

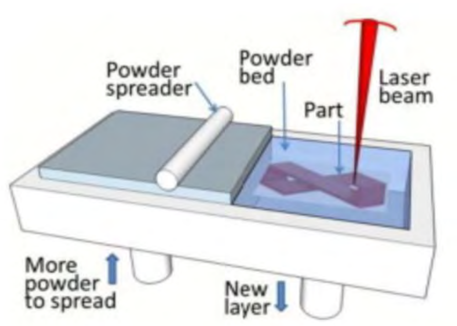

Figure 1. *Process of forming the product [3]*

In our research, the specimen was formed by direct metal laser sintering (DMLS). This procedure is used in several areas, including the field of medicine. In this sector, a basic requirement is that the base material is bio-compatible with the human organism in order to avoid complications after the implant is integrated.

In related research, replacement of a missing part of a skull was completed with DMLS technology. One of the great advantages of AM is the making of custom products. Custom implants can be created by a porous structure that conforms to the geometry of the skull, as shown in Figure 2.

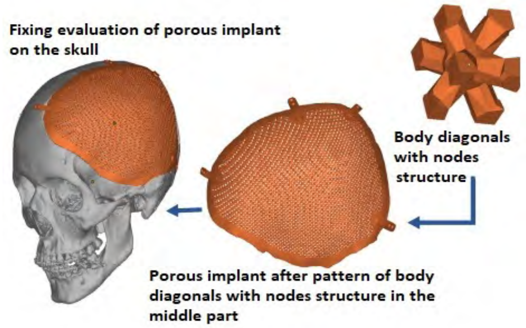

Figure 2. *The shape of the skull implant [4]*

2. Test materials, procedures

The main purpose of our research is to compare the corrosion resistance of two difference test specimens. The first specimen is a Eucatech CCFlex type 4.00x28 mm Co-Cr alloy coronary stent whose base material was produced by conventional powder metallurgy. The second specimen is an EOSINT M280 titanium (Ti-6Al-4V) primary commodity cylindrical body which was made by DMLS. In this case, a Biologic SAS type SP-150 potentiostat was used to measure potential-difference on the two test specimens. The first test used cyclic voltammetry on the stent. Subsequently, the Tafel plot was calculated both on the stent and the titanium specimen. During the measurements 0.9% NaCl physiological saline was used. Before and after the corrosion tests, weight measurement was performed with an APX-200 precision balance and pictures were taken with an Olympus SZX16 stereo-microscope and Zeiss EVO MA10 scanning electron microscope (SEM).

3. Evaluation of results

Table 1. shows the weight loss due to corrosion, which proves the penetration of metal into the solution.

The stereo-microscopic image in Figure 3. shows the surface of the stent before and after the corrosion test. After the measurement, general corrosion was observed on the entire surface of the stent.

Figure 4. shows scanning electron microscopy (SEM) pictures of the stent after the corrosion test.

Table 1. *Weight before and after the corrosion test*

	Before corrosion test	After corrosion test
Co-Cr (L605)	0.0246 g	0.0231 g
Ti-6Al-4V	0.1540 g	0.1539 g

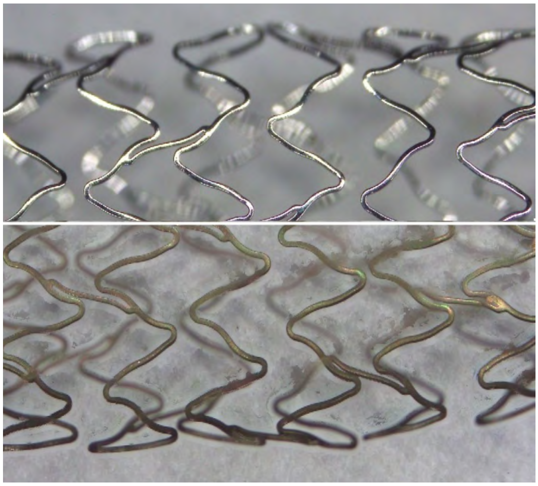

Figure 3. *Surface of the stent before corrosion (above) and after corrosion (below)*

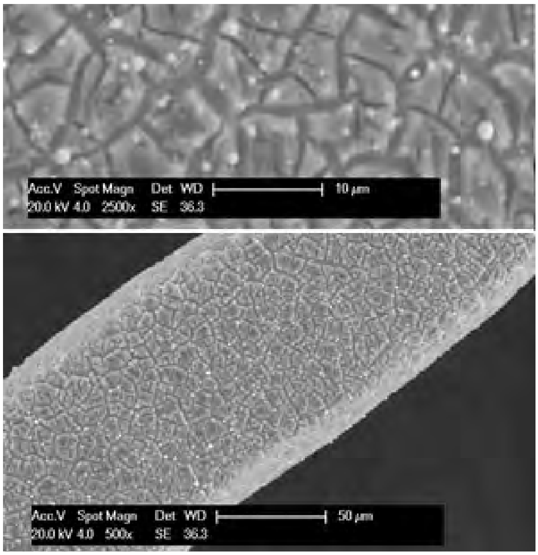

Figure 4. *Scanning electron microscopy images of the stent after the corrosion test*

The stent's base material is made by powder metallurgy, so the tiny white point-like appearances are tungsten-rich segregations, as can be seen in **Figure 4.**

Figure 5. shows the hysteresis curve of cyclic voltammetry and a cathodic and anodic peak potential: E_k = –7.25 mA, E_a = –12.95 mA was determined. In doing so, the passive layer on the stent passes into the solution and a steady state is formed.

Thereafter, the Tafel curve of the stent was determined, as shown in **Figure 6.** After software evaluation with the stent composition, we determined the corrosion rate: $5.72 \cdot 10^{-3}$ mm/year.

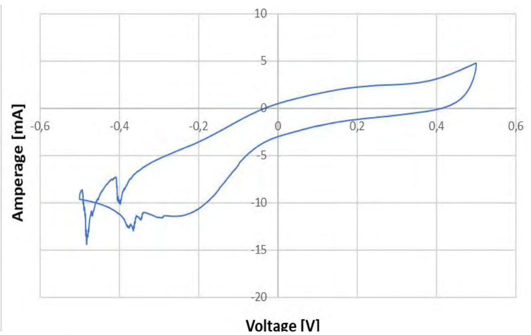

Figure 5. *Cyclic voltammogram of the stent*

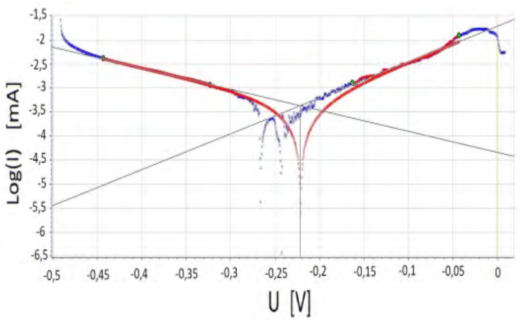

Figure 6. *Tafel plot of the stent*

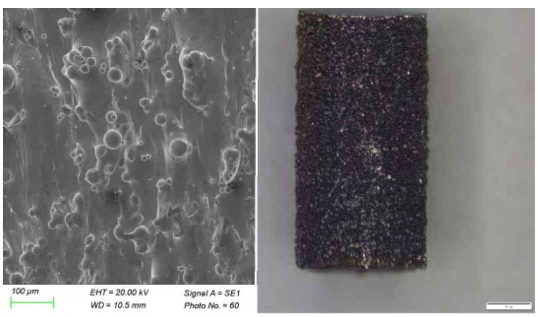

Figure 7. *Titanium cylinder surface SEM (left) and stereomicroscopy (right)*

In **Figure 7.** the SEM and stereomicroscopic image of the additive sample also shows an uneven surface formed by DMLS technology. This uneven surface originated from the melting of the powder material and then random solidification. This microtopography greatly increases the outer surface of the specimen, so the precise surface area is difficult to determine and corrosion processes are affected.

Figure 8. shows that the Tafel curve of the titanium sample differs greatly from the stent Tafel curve. The corrosion rate, in this case, was $2.27 \cdot 10^{-3}$ mm/year.

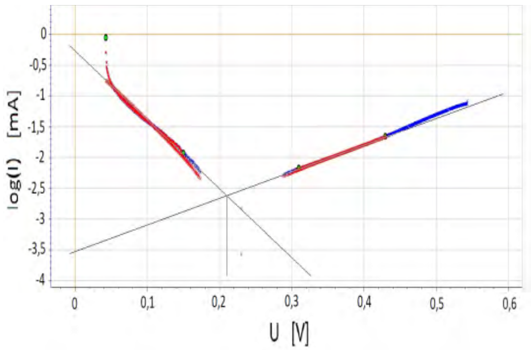

Figure 8. . *Tafel plot of Ti-6Al-4V sample*

4. Conclusions

From the measurement results we can conclude that in the case of NaCl 0.9 % solution, the stent was less resilient with the same corrosion test parameters than the Ti-6Al-4V sample. This is evidenced by the fact that, after corrosion, a relatively large mass decrease was observed in the case of the stent, while in the Ti-6Al-4V sample it was not, and the corrosion rate from the Tafel curve was 2.5 times higher on the stent.

Our test method is appropriate for evaluating additional samples. Among our plans, we compare our results with additive manufactured Co-Cr alloy samples and bulk Ti samples.

Acknowledgements

The project is funded by the National Research, Development and Innovation (NKFIH) Fund. Project title "Developing a new generation of customized medical implants and medical aids for additive technologies". Application ID number: NVKP-16-1-2016-0022. The developers are grateful for the support.

References

[1] Czvikovszky T., Nagy P., Gaál J.: A *polimertechnika alapjai*. Műegyetemi Kiadó, Budapest, 2007.

[2] Gebhardt A.: *Understanding Additive Manufacturing*. Carl Hanser Verlag GmbH & Co. KG, München, 2011.
https://doi.org/10.3139/9783446431621

[3] DebRoy T., Wei H. L., Zuback J. S. et al.: *Additive manufacturing of metallic components – Process, structure and properties*. Progress in Materials Science, 92. (2017) 112–224.
https://doi.org/10.1016/j.pmatsci.2017.10.001

[4] Moiduddin K., Darwish S. et al.: *Structural and mechanical characterization of custom design cranial implant created using additive manufacturing*. Electronic Journal of Biotechnology (2017) 22–31.
https://doi.org/10.1016/j.ejbt.2017.06.005